Proceedings of the ASME 2017 36th International Conference on Ocean, Offshore and Arctic Engineering
OMAE2017
June 25-30, 2017, Trondheim, Norway

OMAE2017-62675

WAVE ENERGY PRIZE EXPERIMENTAL SEA STATE SELECTION

Diana Bull
Water Power Technologies
Sandia National Laboratories
Albuquerque, New Mexico, 87185
Email: Diana.Bull@sandia.gov

Ann Dallman*
Water Power Technologies
Sandia National Laboratories
Albuquerque, New Mexico, 87185
Email: Ann.Dallman@sandia.gov

ABSTRACT

A detailed methodology was used to select the sea states tested in the final stage of the Wave Energy Prize (WEPrize), a public prize challenge sponsored by the U.S. Department of Energy [1]. The winner was selected based on two metrics: a threshold value expressing the benefit to effort ratio (ACE metric) and a second metric which included hydrodynamic performance-related quantities (HPQ). HPQ required additional sea states to query aspects of the techno-economic performance not addressed by ACE. Due to the nature of the WEPrize, limited time was allotted to each contestant for testing and thus a limitation on the total sea states was required. However, the applicability of these sea states was required to encompass seven deployment locations representative of the United States West Coast and Hawaii. A cluster analysis was applied to scatter diagrams in order to determine a subset of sea states that could be scaled to find the average annual power flux at each wave climate for the ACE metric. Four additional sea states were selected, including two highly energetic sea states and two bimodal sea states, to evaluate HPQ. These sea states offer a common experimental testing platform for performance in United States deployment climates.

INTRODUCTION

The characteristics of a deployment location for a Wave Energy Converter (WEC) are often described through a Joint-Probability Distribution (JPD) in which hundreds of sea states comprise the description of the environment. Often, in this representation only the significant wave height (H_s) and period (peak T_p, mean T_0, or energy T_e) are used to define the probability levels. However, the true description of a sea state is much more complex, it involves: spectral shape, peak direction, directional spreading, and other environmental factors like wind, tide, and current. Often, data is not present to characterize all of these aspects. However, even if it were available, developing a multi-dimensional probabilistic understanding of the deployment location is not standard.

The primary purpose of a WEC is to produce as much power as possible at the deployment location in order to reduce the cost of energy given the necessary expenditures to build and operate the WEC farm. Hence when evaluating a deployment location, it is not the probability of a particular sea state occurring that is of primary importance, but rather the energy weighted probability [2], [3] (assuming that a device can produce more power in more energetic environments). The process of evaluating the energy weighted JPD (as a function of H_s and the period of interest) is standard [3] and understandably results in longer wavelength, higher amplitude waves becoming more important.

Experimental testing of a WEC requires prioritization and constraining of the sea states used to comprise a deployment location. A few processes of selecting representative sea states have been proposed (clustering [4], multiple lines of constant wave height and periods [5], or for power variations to be dependent upon changing period only – evaluating constant steepness sweeps), however there has been little convergence by the WEC testing community. Further, these processes have not considered

*Address all correspondence to this author.

TABLE 1: NDBC BUOYS CHOSEN FOR ANALYSIS. NOTE THAT ONLY PARAMETER DATA FROM NDBC WAS CONSIDERED TO KEEP A CONSISTENT FORMAT. (NO DATA FROM CDIP WAS USED.) POR STANDS FOR PERIOD OF RECORD, AS OF 2015.

NDBC #, Location	Depth	Years, POR	Coordinates	AAP Flux in 122 m depth
46083 Glacier Bay, AK	141.4 m	Parameters: 2002-2013, 12 yrs	58.237*N* 137.986*W* (58°14′13"*N* 137°59′8"*W*)	35.5 kW/m
46041 Aberdeen, WA	114.3 m	Parameters: 1988-present, 27 yrs	47.353*N* 124.731*W* (47°21′10"*N* 124°43′50"*W*)	32.7 kW/m
46029 Camp Rilea, OR	144.8 m	Parameters: 1985-present, 30 yrs	46.159*N* 124.514*W* (46°9′32"*N* 124°30′52"*W*)	39.3 kW/m
46050 Newport, OR	128 m	Parameters: 1992-present, 23 yrs	44.639*N* 124.534*W* (44°38′20"*N* 124°32′2"*W*)	37.9 kW/m
46013 Bodega, CA	116.4 m	Parameters: 1981-present, 34 yrs	38.242*N* 123.301*W* (38°14′31"*N* 123°18′2"*W*)	31.5 kW/m
46218 Lompoc, CA	549 m	Parameters: 2005-present, 10 yrs	34.458*N* 120.782*W* (34°27′29"*N* 120°46′56"*W*)	31.2 kW/m
51202 Oahu, HI	82 m	Parameters: 2005-present, 10 yrs	21.414*N* 157.679*W* (21°24′51"*N* 157°40′44"*W*)	16.8 kW/m

the energy weighted probability nor the influence of wishing to evaluate the performance of the WEC in more than one deployment climate.

The Wave Energy Prize (WEPrize) [1] offered a unique opportunity to develop a procedure that could account for multiple deployment locations, the energy weighted probability at those locations, and even the peak direction of the incoming waves. Due to the nature of the WEPrize, limited time was allotted to each contestant for testing and thus a strict limitation on the total number of sea states was required. However, the applicability of these sea states had to encompass seven deployment locations representative of the United States West Coast and Hawaii. This paper describes the procedure used to select six sea states evaluated for the ACE metric as well as the scaling factors associated with each sea state for each of the seven considered deployment locations. In addition, this paper details the selection of the additional four sea states that were used to test the response of devices to other important aspects of sea state parameters.

WAVE ENERGY PRIZE

The Wave Energy Prize was a public prize challenge sponsored by the U.S. Department of Energy (DOE)'s Water Power Program, and details and rules can be found at [1]. The prize was designed to increase the diversity of organizations involved in Wave Energy Converter (WEC) technology development, while motivating and inspiring existing stakeholders. The WEPrize was a three phase competition culminating in a test in the Maneuvering and Seakeeping (MASK) Basin at the Naval Surface Warfare Center (NSWC) Carderock Division in West Bethesda, Maryland. The selection of the winner was based on two metrics: the first a threshold value expressing the *benefit to effort ratio* (the ACE metric) and the second which included hydrodynamic performance-related quantities (the HPQ).

The ACE metric is a low TRL proxy for the levelized cost of energy. The two components that comprise the ratio ACE are:

> Average Climate Capture Width (ACCW) = a measure of the effectiveness of a WEC at absorbing power from the incident wave energy field in units of meters [m],
>
> Characteristic Capital Expenditure (CCE) = a measure of the capital expenditure in commercial production of the load bearing device structure in units of millions of dollars [$M].

The ACE metric is the ratio of ACCW to CCE with a threshold value of 3 m/$M. This paper details the selection of the incident wave fields for which the contestants were evaluated.

Although a scaled wave tank test cannot provide information on all influential parameters (system availability, installation, etc.), it can provide substantial useful information beyond ACE. By requiring additional sensors to monitor other aspects of the device's performance, processing the data to obtain alternative views beyond averages, and subjecting the device to additional wave environments, much more can be learned about a device's overall performance. These hydrodynamic performance-related quantities (HPQ) required additional sea states to query aspects of the techno-economic performance not addressed by ACE. This paper details the selection of these additional HPQ incident wave fields.

MASK Basin

Testing at the MASK basin occured using a Froude-scale factor of 20. The final selection of waves must be able to be produced in the MASK Basin. The MASK is 98.3 m by 61.7 m in area and is 6.1 m deep at the WEPrize testing location.

The new wavemaker can produce multi-directional and short crested seas, multiple sea states at various headings, and synthesize wave grouping and episodic events. The new wavemaker has 216 pivoting paddles along two adjacent sides of the basin. Each paddle is 0.658 m wide, with a hinge depth of 2.5 m [6]. The wavemaker is capable of producing regular waves having a

1/10 slope of 98 cm in height. It can also produce a fully developed seaway (Pierson-Moskowitz spectral distribution) of 35 cm in significant wave height and high steepness focused waves of 50 cm in significant height [6].

DEPLOYMENT LOCATIONS

Sea states that are representative of the U.S. Pacific West Coast and Hawaii wave climates were selected. Specific locations were chosen based on the desire to have a mixture of predominant incoming environments, good spatial distribution, at least seven years of data, and also locations that have been considered as probable for the development of WEC farms. The West Coast of the United States is the target area for large-scale commercial production of wave power, and is of primary importance. However, device performance in early market opportunity locations with high utility costs, such as Hawaii and Alaska, was also of interest to include. The buoys used for data analysis are detailed in Table 1. Buoys near the 100 m contour line were most desirable but not available in all locations. All average annual power flux values were calculated for a single depth of 122 m since each of the deployment locations were to be tested in the MASK basin (122 m is twenty times the testing depth in MASK for the Prize).

Sea state parameters reported by NDBC were used to analyze the wave climate at each buoy. The significant wave height reported by NDBC (and used here) is the average of the highest one-third of all the wave heights during a 20-minute sampling period. The peak period is the period with maximum energy in the spectrum. Lastly, the peak direction was used to determine relative wave scatter diagrams for each of the deployment locations except Glacier Bay (no directional data was available from that buoy).

The scatter diagrams of H_s vs T_p for occurrence and percentage of total energy were calculated and are shown as subplots for Newport, OR in Figure 1. The top subplot in Figure 1 shows the percent occurrence of each binned sea state. The lower subplot in Figure 1 shows the percentage of total energy that each sea state contributes.

There are empty bands of T_p in the JPDs, for example from $15\,\text{s} \leq T_p < 16\,\text{s}$, because some of the lower frequencies recorded by NDBC are uniformly spaced, which correspond to greater spaced peak periods. For example, although the frequencies recorded by NDBC changed over the years, some of the frequencies recorded by NDBC over the POR are 0.06 Hz, 0.0625 Hz, 0.0675 Hz which correspond to periods of 16.67 s, 16 s, 14.81 s. Therefore no data will be in the bin $15\,\text{s} \leq T_p < 16\,\text{s}$.

Some of these buoys did have spectral data available. This information could have been used to investigate spectral shapes as well as directional spreading characteristics. Spectral data was not analyzed for the creation of the sea states used in the WEPrize due to time constraints.

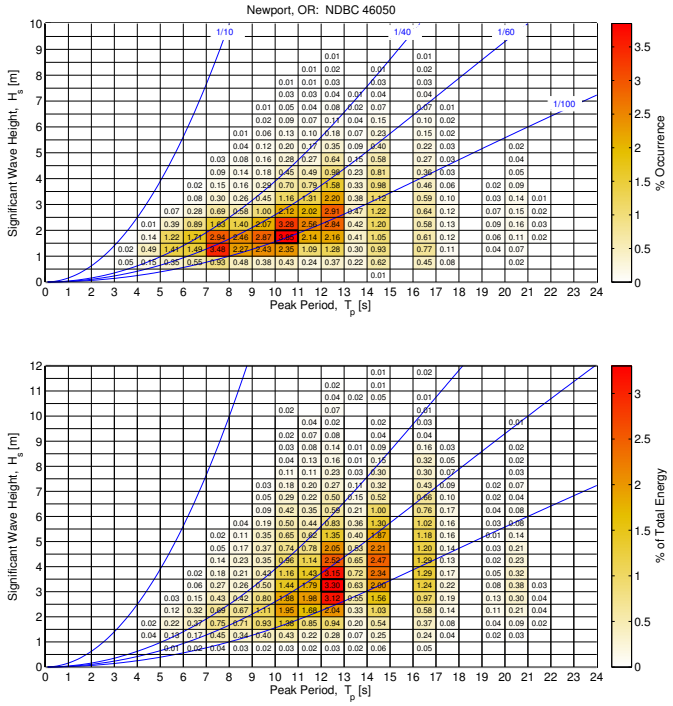

FIGURE 1: OCCURENCE AND ENERGY SCATTER DIAGRAMS FOR NDBC 46050, NEWPORT, OREGON.

SEA STATE SELECTION: K-MEANS ALGORITHM

Following the work of [4] a cluster analysis was applied to scatter diagrams in order to determine a subset of sea states that could be scaled to find the average annual power (AAP) flux. This subset is found via minimization of the squared Euclidian distance between each point and a cluster centroid. This k-means clustering procedure is a built-in MATLAB algorithm within the Statistics Toolbox; the user defines the number of clusters over which the optimization should take place. An iterative partitioning method optimizes the centroid of each cluster and the cluster size by minimizing the sum of point-to-centroid distances, summed over all k clusters. Hence, each sea state is assigned to an optimally determined cluster centroid that has the minimum point-to-centroid cluster distance.

The k-means clustering algorithm can be used on either the occurrence or energy occurrence scatter diagrams. As discussed in the Introduction, the energy occurrence is of primary importance for WECs and thus this analysis focuses on the application of k-means clustering on the energy occurrence scatter diagrams. Figure 2 shows the optimal assignments for six clusters when analyzing the energy occurrence scatter diagram for Newport, OR. The details of the cluster centroids and scalings are given in Table 2.

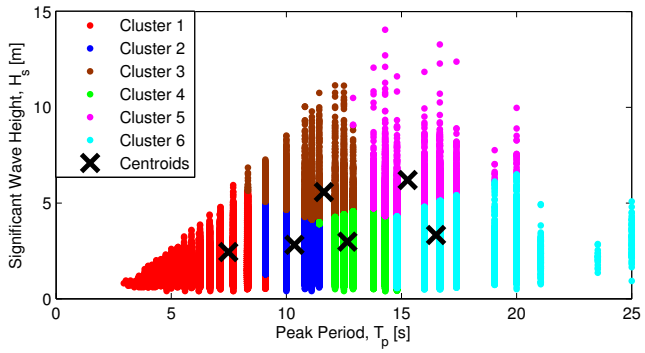

FIGURE 2: CLUSTERING EXAMPLE USING K-MEANS FOR NDBC 46050, NEWPORT, OR, USING THE ENERGY OCCURRENCE SCATTER DIAGRAM. THE AVERAGE ANNUAL POWER (AAP) FLUX AT THE BUOY'S DEPLOYMENT DEPTH IS 37.8 kW/m.

Cluster	T_p	H_s	Power Flux	Ξ_{ini}	Weighted Power $Flux_{ini}$	Ξ	Weighted Power Flux
	sec	m	kW/m	%	kW/m	%	kW/m
1	7.60	2.39	18.2	0.079	1.44	0.163	2.98
2	10.66	2.73	33.6	0.217	7.30	0.244	8.21
3	11.57	5.74	162.	0.147	23.8	0.034	5.56
4	13.32	3.23	60.5	0.293	17.7	0.183	11.1
5	15.19	6.09	251.	0.147	36.9	0.022	5.55
6	17.62	3.59	105.	0.117	12.3	0.042	4.41

TABLE 2: K-MEANS CLUSTER ANALYSIS ON ENERGY OCCURRENCE SCATTER DIAGRAM AND SUBSEQUENT ADJUSTMENTS TO THE SCALING FACTORS. THE SUM OF THE WEIGHTED POWER VALUES USING Ξ RESULTS IN AN AAP FLUX OF 37.8 kW/m WHICH MATCHES THE AAP AT THE BUOY'S DEPLOYMENT DEPTH.

The goal of the clustering analysis is to obtain the average annual power flux for each deployment location using a small subset of the sea states that comprise the scatter diagram. As would be expected, the sum of the all of the occurrences within the identified cluster boundaries to identify the initial scaling factor Ξ_{ini} for that cluster combined with the omnidirectional power fluxes results in incorrect average annual power fluxes for the deployment location. In fact, the sum of the weighted power flux values using Ξ_{ini} results in an average annual power (AAP) flux of 99.5 kW/m. Thus, the scaling for each cluster must be calculated in a distinct way such that the total occurence weighted power flux within that cluster is represented. In this method, the occurrence weighted power flux was calculated by summing the product of the probability of occurrence with the power flux for all data points within the cluster boundaries for each energy occurrence cluster. This value divided by the power flux of the centroid determines the correct scaling factor for the centroid. For example, Cluster 3 in Table 2 contributes a total of 5.56 kW/m of power flux to the average annual power flux of 37.8 kW/m. Given that this centroid's omnidirectional power flux is 162 kW/m this procedure then dictates that the adjusted scaling Ξ should be the ratio of these two values to obtain 0.034. These adjustments ensure that the average annual power flux would be obtained from the sum of all the centroids power flux multiplied by their adjusted scaling factors.

Another important facet of this technique is that centroid location can be altered and the cluster to be associated with the newly altered centroid can be recalculated. The cluster points are again selected through minimization of the squared Euclidian distance using the built in MATLAB function *pdist2*. Hence, not only can the cluster centroids be assigned using the k-means algorithm, they can also be selected and the most optimal cluster can then be associated with them using the same squared Euclidian distance as the minimization parameter.

These two techniques, optimal assignment of the centroid and optimal assignment of the cluster given a centroid definition, will be used in concert in the following sections to determine the single set of six sea states used to describe all seven deployment locations.

COALESCENCE OF DEPLOYMENT LOCATIONS

For the tank testing, a limited number of common sea states must be chosen and these should represent the wave climates at the seven selected sites. A common set of sea states can be given site-specific scaling factors in order to represent the climate at each site. It was desired to have the scaling factors reflect the annual average power at each site as well.

A single set of sea states

The cluster analysis described above was used to find the optimal set of six sea states (or centroids in this method) for each deployment location using the energy occurrence scatter diagrams. This analysis revealed seven distinct optimizations as shown in Table 3, however one set of centroids was needed to represent all seven deployment locations. Coalescing of these sea states required multiple iterations to ensure that no individual sea state (or set of sea states) represented more than ∼30% of the annual average power flux, i.e. that the distribution of contribution to the average annual power flux was even as opposed to highly peaked towards individual sea states.

In the first iteration to coalesce the sea states, similar centroids among the buoys were averaged to find possible common

TABLE 3: THE SIX CLUSTER CENTROIDS FOUND USING K-MEANS CLUSTERING ON THE ENERGY OCCURRENCE SCATTER DIAGRAM FOR EACH DEPLOYMENT LOCATION.

Glacier Bay, AK		**Aberdeen, WA**		**Camp Rilea, OR**		**Newport, OR**		**Bodega, CA**		**Lompoc, CA**		**Oahu, HI**	
T_p	H_s	T_p	H_s	T_p	H_s	T_p	H_s	T_p	H_s	T_p	H_s	T_p	H_s
s	**m**	**s**	**m**	**s**	**m**	**s**	**m**	**s**	**m**	**s**	**m**	**s**	**m**
7.30	2.72	9.28	2.35	9.76	2.48	7.60	2.39	7.51	2.54	7.74	2.37	6.21	1.87
10.30	2.87	11.82	4.98	11.59	4.75	10.66	2.73	10.09	2.85	9.86	2.83	7.50	2.12
12.07	3.74	12.21	2.82	13.51	3.27	11.57	5.74	12.18	3.00	12.40	2.93	9.10	2.34
12.10	5.99	15.28	3.37	13.76	6.69	13.32	3.23	14.28	2.91	15.03	4.39	11.13	2.49
15.09	7.10	15.40	6.41	16.81	6.37	15.19	6.09	15.42	5.21	15.42	2.32	12.95	2.36
15.38	3.83	20.34	3.66	17.43	3.18	17.62	3.59	17.80	3.07	18.94	3.31	15.59	2.44

centroids. This method was completed with the intent to minimize the standard deviations in the average and hence represent the commonalities; in some instances, outliers were removed to adhere to this goal. Six of the buoys had a centroid within 6-8 s and 1.5-3 m thus producing the first common centroid. Seven of the buoys had a centroid within 9-11 s and 2-3 m, so these were averaged, arriving at the second common centroid. For all the buoys there was either a centroid within 11.5-13 s with a large H_s (>4 m), or one within 11.5-13 s with a smaller H_s (<4 m), and some buoys had both. Therefore, the four centroids with 11.5-13 s and large H_s were averaged, to arrive at the third common centroid. Next, the five centroids with 11.5-13 s and smaller H_s were averaged, arriving at the fourth common centroid. Five of the buoys had centroids between 15-16 s with large H_s (>4 m), so these were averaged for the fifth common centroid. Finally, there were various centroids among the buoys with larger periods (>16 s) and H_s between 2-4 m, that were desired to represent the sixth common centroid. However, combining this spread of periods resulted in a large standard deviation of T_p (~ 2 s). In addition, the wave tank is limited to maximum periods (at full scale) of about 16-17 s. Therefore, the peak period for the sixth common centroid was set given the tank limitations. The results of this first iteration are shown in Table 4.

After this initial set of common centroids was found, small alterations were made to the centroid centers. Each of these alterations had a unique purpose: increasing spread between peak periods, achieving centroid centers on approximately constant bulk steepness lines, and to ensure that no centroid was dominate (in terms of its contribution to the average annual power flux at the deployment location) across multiple deployment locations. Centroids 3 and 4 were the targets of these iterations. The updated set of centroids are shown in Tables 5 and 6. With these adjustments average bulk steepness values over the deployment

TABLE 4: THE FIRST SET OF COMMON CENTROIDS.

Cluster	T_p	H_s	**N**	**std. dev.** T_p	**std. dev.** H_s
	s	**m**		**s**	**m**
1	7.31	2.34	6	0.56	0.30
2	9.86	2.64	7	0.55	0.24
3	11.77	5.36	4	0.25	0.59
4	12.36	2.97	5	0.35	0.50
5	15.23	5.84	5	0.18	1.06
6	16.50	3.25	10	N/A	0.51

locations for each centroid are 1/35.6, 1/57.5, 1/38.6, 1/122.4, 1/60.4, 1/124.9. Further these adjustments have resulted in no centroid dominating the contribution to average annual power flux; centroids 3 and 4 are more predominate in multiple deployment locations but are not dominate across all or individually dominate over other centroids within a deployment location. Therefore, the centroids in Tables 5 and 6 were determined to be appropriate for the WEPrize sea state selection. Note that the sum of the adjusted weighted power flux in Tables 5 and 6 matches the AAP of each buoy, assuming the common depth of 122 m rather than each buoy's deployment depth.

Directionality of the sea states

The process of choosing appropriate directions for the common centroids required creative analysis not seen before. The most probable directions along with the contribution to average annual power flux were used as optimization variables. In this

TABLE 5: THE FINAL SET OF CENTROIDS, AND THE ASSOCIATED POWER, STEEPNESS, SCALING FACTORS, WEIGHTED POWER, AND PERCENT OF AVERAGE ANNUAL POWER FOR GLACIER BAY, ABERDEEN, AND CAMP RILEA LOCATIONS.

	T_p	H_s	Power Flux	Steepness^{-1}	Ξ	Weighted Power Flux	Contribution to AAP Flux
	s	m	kW/m	λ_{T_p}/H_s		kW/m	%
Glacier Bay, AK	7.31	2.34	16.7	35.6	0.243	4.07	11
	9.86	2.64	29.0	57.5	0.332	9.62	27
	11.52	5.36	141.1	38.6	0.075	10.59	30
	12.71	2.05	23.1	122.4	0.200	4.61	13
	15.23	5.84	233.5	60.4	0.024	5.61	16
	16.50	3.25	79.8	124.9	0.012	1.00	3
						35.5	
Aberdeen, WA	7.31	2.34	16.7	35.6	0.137	2.29	7
	9.86	2.64	29.0	57.5	0.277	8.03	25
	11.52	5.36	141.1	38.6	0.041	5.82	18
	12.71	2.05	23.1	122.4	0.338	7.80	24
	15.23	5.84	233.5	60.4	0.022	5.19	16
	16.50	3.25	79.8	124.9	0.045	3.56	11
						32.7	
Camp Rilea, OR	7.31	2.34	16.7	35.6	0.155	2.60	7
	9.86	2.64	29.0	57.5	0.307	8.88	23
	11.52	5.36	141.1	38.6	0.056	7.88	20
	12.71	2.05	23.1	122.4	0.344	7.94	20
	15.23	5.84	233.5	60.4	0.037	8.63	22
	16.50	3.25	79.8	124.9	0.042	3.35	9
						39.3	

TABLE 6: THE FINAL SET OF CENTROIDS, AND THE ASSOCIATED POWER, STEEPNESS, SCALING FACTORS, WEIGHTED POWER, AND PERCENT OF AVERAGE ANNUAL POWER FOR NEWPORT, BODEGA, LOMPOC, AND OAHU LOCATIONS.

	T_p	H_s	Power Flux	Steepness^{-1}	Ξ	Weighted Power Flux	Contribution to AAP Flux
	s	m	kW/m	λ_{T_p}/H_s		kW/m	%
Newport, OR	7.31	2.34	16.7	35.6	0.175	2.93	8
	9.86	2.64	29.0	57.5	0.268	7.77	20
	11.52	5.36	141.1	38.6	0.058	8.12	21
	12.71	2.05	23.1	122.4	0.295	6.80	18
	15.23	5.84	233.5	60.4	0.034	8.00	21
	16.50	3.25	79.8	124.9	0.054	4.29	11
						37.9	
Bodega, CA	7.31	2.34	16.7	35.6	0.207	3.47	11
	9.86	2.64	29.0	57.5	0.230	6.67	21
	11.52	5.36	141.1	38.6	0.012	1.64	5
	12.71	2.05	23.1	122.4	0.466	10.76	34
	15.23	5.84	233.5	60.4	0.016	3.85	12
	16.50	3.25	79.8	124.9	0.064	5.08	16
						31.5	
Lompoc, CA	7.31	2.34	16.7	35.6	0.152	2.54	8
	9.86	2.64	29.0	57.5	0.270	7.81	25
	11.52	5.36	141.1	38.6	0.014	2.00	6
	12.71	2.05	23.1	122.4	0.391	9.03	29
	15.23	5.84	233.5	60.4	0.010	2.24	7
	16.50	3.25	79.8	124.9	0.095	7.61	24
						31.2	
Oahu, HI	7.31	2.34	16.7	35.6	0.328	5.49	33
	9.86	2.64	29.0	57.5	0.245	7.09	42
	11.52	5.36	141.1	38.6	0.001	0.10	1
	12.71	2.05	23.1	122.4	0.133	3.07	18
	15.23	5.84	233.5	60.4	0.000	0.03	0
	16.50	3.25	79.8	124.9	0.013	1.06	6
						16.8	

analysis individual peak direction is not used; all peak directions are relativized to the head direction and the degree of off-head is quantified in increments of 10°. The head direction for each deployment location is established by determining the most probable direction overall; these are identified in Table 7.

Given these head directions, the quantification of off-head change for each bin in the occurrence scatter diagram was established. Figure 3 illustrates this analysis; the head direction is now taken to be 0° and the quantification of off-head is shown in increments of ±10°. In this manner, if a bin in the Newport, OR deployment location had an off-head of - 10°, it would represent a peak incident direction of 275° because the most probable peak incident direction is 285°. Relativizing the directions in this manner is necessary to compare such spatially disparate sites, but also seen as reasonable because directionally sensitive WECs would most likely be aligned to the predominate direction.

For each deployment location this relativization of direction was completed. Then, using the six common cluster boundaries, the omnidirectional power flux associated with each off-head bin in that cluster was summed, i.e. all H_s-T_p elements with an off-head value of - 10°, in Cluster 1, for instance, had their omnidirectional power flux summed and normalized by the AAP flux in the deployment location. Figure 4 illustrates the results for the common centroids at each deployment location. This analysis illuminates the importance of an off-head direction to the contribution of power flux within that cluster. In fact, this analysis clearly shows that, for some cases, the same centroid should be run with multiple directions since a significant portion of the power flux is spread over more than one direction.

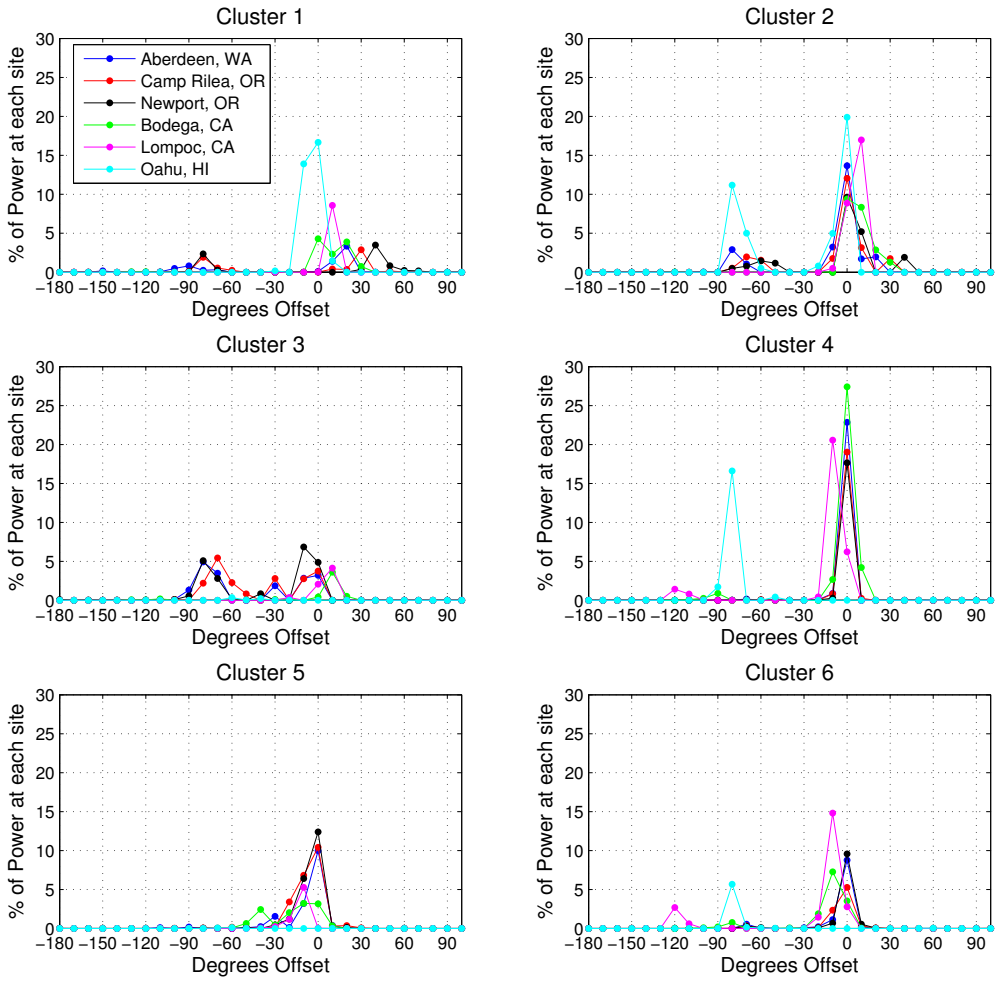

FIGURE 4: THE % OF POWER AT EACH SITE FOR EACH DIRECTION OFFSET IS GIVEN, FOR EACH CLUSTER.

Since Figure 4 was unable to clearly highlight which cluster should be associated with a particular off-head direction or even what that off-head direction should be, an additional analysis step was needed. In this method the total contribution to power flux for off-head direction is analyzed as opposed to looking at the clusters independently. Additionally, all deployment locations are summed together in order to get a very high-level understanding of which off-head directions are contributing and at what percentage to the average annual power flux. Figure 5 shows this high-level analysis in which it is clear that most of the incident power flux is from head with small off-head deviations ($\pm 10°$) with one strongly off-head significant contribution to power. In fact, 11.2% of the total combined power flux contribution is in the offset directions - 80° to -70°, 18.3% is in - 10°, 46.2% is in 0°, and 10.6% is in 10°.

By then evaluating the percentage of annual average power flux each cluster contributes for each deployment location (right hand column of Tables 5 and 6) it is possible to assign off-head directions to the centroid that contributes (on average) the same percentage of annual average power flux. The - 80° / - 70° offset direction represents about 11.2%, so it was assigned to cluster 3 which contributes on average 11.7% to the deployment location annual average power flux. The - 10° offset direction represents 18.3%; the cluster with the closest percentage is cluster 4. The + 10° offset direction represents 10.6%, so it was assigned to cluster 1. The rest of the clusters were assigned 0°. To then ensure that these associations do not contradict the location and cluster specific analysis first presented, visual inspection of Figure 4 solidifies the cross-verification.

Summary of selected waves

The results of the k-means clustering analysis and directional analysis resulted in a set of six sea states that can be produced in the MASK Basin. There are at least five parameters

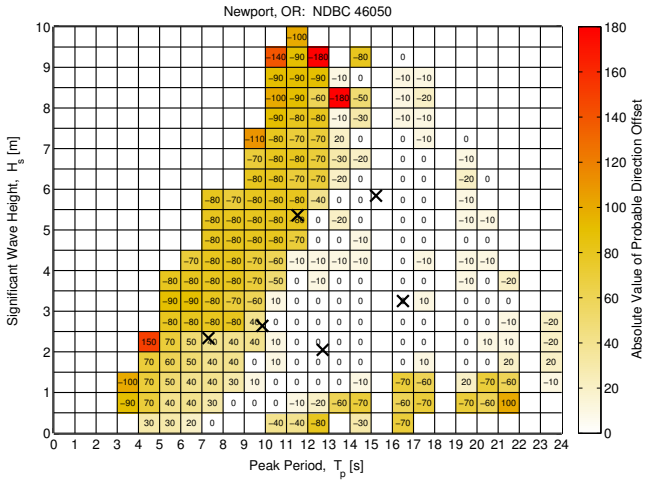

FIGURE 3: THE DIRECTION OFFSET FROM THE MOST PROBABLY IS SHOWN FOR EACH H_s, T_p BIN FOR NDBC 46050. THE SIX COMMON CENTROIDS ARE MARKED WITH AN X.

TABLE 7: MOST PROBABLE PEAK INCIDENT DIRECTION FOR EACH DEPLOYMENT LOCATION.

Location	Direction from N
Glacier Bay, AK	–
Aberdeen, WA	285°
Camp Rilea, OR	285°
Newport, OR	285°
Bodega, CA	295°
Lompoc, CA	305°
Oahu, HI	75°

required to sufficiently describe a sea state: period, significant waveheight, peakedness / bandwidth of the spectral shape, heading, and directional spreading. A full description of the sea states' parameters are given in Table 8. The spectrum is described through the Bretschneider standard format in Equation 1 (also known as ISSC or modified Pierson-Moskowitz), where the peakedness (or peak enhancement factor), γ, is always 1.

$$S(f) = 5/16\, H_s^2\, f_m^4\, f^{-5}\, exp(-5/4\, [f/f_m]^{-4}) \qquad (1)$$

where f is frequency in Hz, f_m is the peak frequency ($= 1/T_p$), and H_s is the significant wave height in meters.

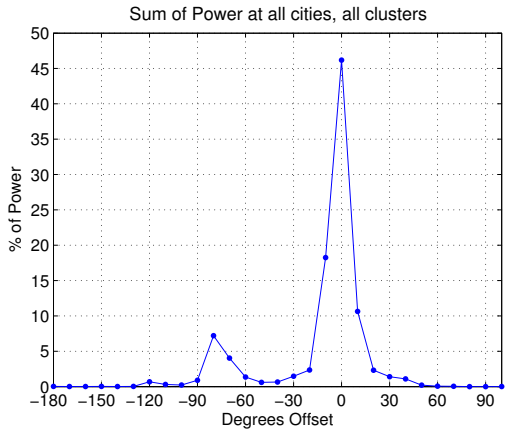

FIGURE 5: THE % OF POWER FLUX OVER ALL CLUSTERS AND ALL BUOY LOCATIONS GIVEN AS A FUNCTION OF DIRECTIONAL OFFSET FROM THE MOST PROBABLE DIRECTION.

ADDITIONAL WEPRIZE SEA STATES

The sea states used to calculate the ACE metric assume a simple spectral shape and no directional spreading. Additionally, the performance of a WEC in highly energetic sea states or sea states with unusual spectral shapes can be very different than in the sea states identified in Table 8. Hence, four additional sea states were tested in the final stage gate of the WEPrize. Although the selection of these additional four sea states was based on information from the deployment climate, their selection did not result from a statistical analysis of any particular deployment location. Instead these were selected to test the devices in sea states that explored more fully the parameters that can be used to alter the energy distribution available to the devices. The performance of the devices in these additional sea states were used to compute the HPQ factors which weighted the ACE metric.

The first set of additional sea states tested the devices' response in highly energetic seas. Table 9 summarizes the parameters describing these waves. Not only has the spectral shape changed for these sea states, but additionally directional spreading was associated with the waves. The headings were chosen loosely off of the directional analysis shown in Figures 4 and 5. Further, storms tend to have disparate incident directions from operational waves, hence two strongly off-head directions were chosen. The omnidirectional power fluxes for these two sea states is $\sim$3 times larger than the ACE sea states, but the two are also very close to one another. This difference in bulk steepness for similar incident power flux was intentionally testing the devices sensitivity to bulk steepness.

The second set of additional sea states tested the devices' response to bimodal seas. The motivation for these seas was two-fold: the Northwestern shore of the US has bimodal char-

TABLE 8: DETAILED PARAMETERIZATION OF THE SIX SEA STATES CHOSEN TO REPRESENT SEVEN DEPLOYMENT CLIMATES FOR THE WEPRIZE COMPETITION.

Cluster	T_p	H_s	peakedness	heading	spreading $\cos^{2s}$	Power Flux	Steepness^{-1}
	sec	m	γ	deg	s value	kW/m	λ_{T_p}/H_s
1	7.31	2.34	1.0	10	inf	16.7	35.6
2	9.86	2.64	1.0	0	inf	29.0	57.5
3	11.52	5.36	1.0	-70	inf	141.1	38.6
4	12.71	2.05	1.0	-10	inf	23.1	122.4
5	15.23	5.84	1.0	0	inf	233.5	60.4
6	16.50	3.25	1.0	0	inf	79.8	124.9

TABLE 9: LIWS: ENERGETIC SEA STATES SPECIFIED WITH DIRECTIONAL SPREADING, OFF-HEAD, AND WITH A NARROW SPECTRUM.

Parameter	Unit	LIWS1	LIWS2
T_p	sec	13.9	11.2
H_s	m	7.9	9.2
peakedness	γ	3.3	3.3
heading	deg	-30	-70
spreading $\cos^{2s}$	s value	3	7
Omni Power Flux	kW/m	406	426
Steepness^{-1}	λ_{T_p}/H_s	38	21

acteristics, as does Hawaii ([7] & [8]), and given that not all data buoys collect information on the spectral shape, the likelihood of mis-characterizing the deployment spectral shape is high. Thus two of the sea states (2 and 4 from Table 8 which occur with high weighting for each site) were used as the combined wave properties for two distinct bimodal spectra following the procedure laid out by Mackay [8]. Table 10 summarizes the combined and bimodal properties. Note, the energy content in the bimodal equivalents of their parent waves is not exactly the same due to differences in the spectral bandwidth paramter γ, however it is still extremely close.

The wind and swell sides (only indicative of the lower and higher frequency partitions respectively) of the bimodal spectra were weighted distinctly in terms of their contribution to total incoming power. The determination of these weightings follow the conservation of power principles laid out by Mackay [8] in which the normalized periods, omnidirectional powers, and steepnesses can all be expressed in terms of separation (dT_n) between normalized periods and the normalized significant wave heights H_{sn} and H_{wn}. The normalized parameters for each partition are found by taking the "unimodal" properties of the partition divided by the combined wave properties (e.g. $H_{sn} = H_{ss}/H_s$). Hence, by determining the separation and the normalized significant wave-height the following can be shown:

$$T_{sn} = 1 + H_{wn}^2 dT_n, \quad T_{wn} = 1 + H_{sn}^2 dT_n \tag{2}$$

$$P_{sn} = H_{sn}^2 T_{sn}, \quad P_{wn} = H_{wn}^2 T_{wn}. \tag{3}$$

In addition to these wind and swell characteristics, each partition had distinct headings and directional spreading properties associated with it. Again, this not only showcased the incredible capabilities of the MASK Basin but it also enhanced the testing campaign to create the most realistic seas that the devices could potentially encounter. Good performance in these seas would be indicative of a device that would perform well in the real ocean.

CONCLUSIONS

This paper has detailed the methods and analysis behind the selection of both the experimental ACE and HPQ sea states for the WEPrize competition. Six sea states were chosen to represent seven distinct deployment climates of interest on the West Coast of the United States. The k-means clustering method was used to identify the best cluster definitions from the energy occurrence scatter diagrams. The same minimization technique (squared Euclidian distance) was then used to define the cluster boundaries for the six common sea states to all seven deployment locations. Scaling factors (Ξ) were determined such that the scaled centroids would sum to the expected average annual power flux (in 122 m water depth) for each deployment location. Additionally, the methodology behind selection of the incident direction for

these long-crested sea states was detailed. The directions associated with the sea states align with an overall directional-energy analysis for all seven deployment climates.

The HPQ sea state selection was also described in this paper. These sea states are intended to represent more fully the available energy distributions in deployment climates. Highly energetic waves with directional spreading, while not strictly representative of high return period storms, were intended to test the devices performance in stormy conditions. Bimodal spectra incident from distinct directions with spreading were intended to create the most realistic waves that a device could experience. These additional HPQ sea states took full advantage of the incredible capabilites of the newly updated MASK basin.

The ACE and HPQ sea states have established a set of standard conditions that nine devices have been tested against in the WEPrize. These sea states offer a common experimental testing platform for performance in United States deployment climates.

TABLE 10: RWS: REALISTIC SEA STATES SPECIFIED WITH A BIMODAL SPECTRUM, DIRECTIONAL SPREADING, AND FROM DISTANT DIRECTIONS.

			Cluster 2 dT_n=0.75 H^2_{sn}=33% H^2_{wn}=67%	**Cluster 4** dT_n=0.5 H^2_{sn}=60% H^2_{wn}=40%
Swell Side	T_p	sec	14.38	14.83
	H_s	m	1.52	1.59
	peakedness	γ	2	2
	heading	deg	-70	-70
	spreading $\cos^{2s}$	s value	7	7
	Omni Power Flux	kW/m	15.1	17.1
	Steepness^{-1}	λ_{T_p}/H_s	209	211
Wind Side	T_p	sec	7.18	8.65
	H_s	m	2.16	1.30
	peakedness	γ	2	2
	heading	deg	0	-10
	spreading $\cos^{2s}$	s value	10	10
	Omni Power Flux	kW/m	14.5	6.29
	Steepness^{-1}	λ_{T_p}/H_s	37	90

ACKNOWLEDGMENT

This work was funded by the U.S. Department of Energy's Wind and Water Power Technologies Office. Sandia National Laboratories is a multi-mission laboratory managed and operated by Sandia Corporation, a wholly owned subsidiary of Lockheed Martin Corporation, for the U.S. Department of Energy's National Nuclear Security Administration under contract DE-AC04-94AL85000. Helpful conversations were had with Jochem Weber on the directional analysis.

REFERENCES

[1] 2016. EERE. Wave Energy Prize, U.S. Department of Energy [Online]. Available: http://waveenergyprize.org/

[2] Cahill, B. and Lewis, T., "Wave Energy Resource Characterization and the Evaluation of Potential Wave Farm Sites," in OCEANS 2011, Hawaii, Sep. 2011.

[3] Dallman, A.R. and Neary, V.S., "Characterization of U.S. Wave Energy Converter (WEC) Test Sites: A Catalogue of Met-Ocean Data, 2nd Edition." Sandia National Laboratories (SNL-NM), Albuquerque, NM (United States), Tech. Rep., 2015.

[4] Lavelle, J. and Kofoed, J. P., "Representative spectra of the wave resource from sea wave measurements," in EWTEC, Aalborg, Denmark, 2013.

[5] Holmes, B., 2009. *Tank testing of wave energy conversion systems: marine renewable energy guides.* European Marine Energy Centre.

[6] OCEAN WAVES WORKSHOP 2015. Session 3 Presentation-The Harold E. Saunders Maneuvering and Seakeeping (MASK) Facility New Directional Wavemaker, no. Paper 3, University of New Orleans. http://scholarworks.uno.edu/oceanwaves/2015/Session3/3

[7] Lenee-Bluhm, P., 2010. The wave energy resource of the US Pacific Northwest. MS thesis, Univ. of Oregon, Corvalis.

[8] Mackay, E. B., 2011. Modelling and description of omnidirectional wave spectra. In Proceedings of the 9th European Wave and Tidal Energy Conference (EWTEC 2011), pp. 122–131.